Modeling and Kinetics of Allylation of Phenol in a Triphase-Catalytic Membrane Reactor

Ho-Shing Wu and May-Huey Lo
Dept. of Chemical Engineering and Material Science, Yuan-Ze University, ChungLi, Taoyuan, 32026, Taiwan

DOI 10.1002/aic.10361
Published online in Wiley InterScience (www.interscience.wiley.com).

The reaction of allyl bromide with phenol, in the presence of quaternary methyl ammonium membrane in a 1,2-dichloroethane/aqueous solution in a membrane reactor, was investigated. The reaction mechanism of this system was described by combining the experimental data and Langmuir–Hinshelwood theory. Theoretical models and calculations were performed to predict the kinetic behavior of the reaction system. Experimental results confirmed the developed model. The parameters of selectivity coefficient, adsorbing rate constant, and activation energy were obtained. © 2005 American Institute of Chemical Engineers *AIChE J,* 51: 960–970, 2005
Keywords: reactor design, reaction kinetics, phase-transfer catalysis, triphase, anion-exchange membrane

Introduction

Liquid–liquid phase-transfer catalysis (PTC) is an effective tool for synthesizing organic chemicals from two immiscible reactants.[1-3] Most PTC reactions are carried out on an industrial scale in the batch mode in mixer–settler arrangements. However, the process of using a two-phase phase-transfer catalytic reaction always encounters the problem of separation and purifying the final product from the catalyst. Although the catalyst can be separated from the product by methods of either distillation or extraction, the operating cost is increased and the purity of product is reduced.

In view of reactor design in a triphasic reaction, Ragaini and coworkers[4-7] emphasized the importance of effluent recycle concept in the fixed-bed reactors with a recycling pump or with a recycling pump and an ultrasonic mixer. That is, their reactor type was a total recycle reactor, not a continuous reactor. Schlunt and Chau[8] reported the use of a cyclic slurry reactor, which allowed the immiscible reactants to contact the catalyst sites in controlled sequential steps. Wu and Wang[9] proposed the slurry reactor and fixed-bed reactor to evaluate a liquid–solid–liquid reaction. However, for triphase reactions in liquid–liquid systems where the catalyst is a solid phase, the reactor type used in this reaction system is not a clear solution. From all the triphase catalytic displacement reaction results, in general, the optimum reaction conditions would require (1) very small particles to reduce intraparticle diffusional effects, (2) low crosslinked density to enhance solvent swelling, (3) a good swelling solvent, (4) a turbulently agitated reactor to eliminate external mass transfer effects, and (5) a method of separating the catalyst. Thus, the solid catalyst of a polymer-supported resin has restricted the industrial application in a phase-transfer catalyzed reaction.

When the catalyst is immobilized within the pores of an inert membrane, the catalytic and separation functions are engineered in a very compact fashion. If the catalyst is inside the pores of the membrane the combination of the open pore path and transmembrane pressure provides easier access of the reactants to the catalyst. The membrane system offers the advantages of (1) separating the catalyst from the reaction matrix, (2) keeping the phases apart to minimize the potential for forming emulsions, and (3) high surface area per unit volume of reactor. Furthermore, Zaspailis et al.[10] estimated that a membrane catalyst could be 10 times more active than that in the form of catalyst pellets. The membrane system as listed in Table 1 was previously studied in the phase-transfer–catalytic reaction. Stanley and Quinn[11] reported a membrane reactor using tetra-*n*-butyl ammonium bromide (TBAB) as the homogeneous catalyst, which operated in the continuous mode. Grigoropoulou et al.[12] reported the selective oxidation of ben-

Correspondence concerning this article should be addressed to H.-S. Wu at cehswu@saturn.yzu.edu.tw.

Table 1. Comparison of Membrane Reaction System

Reference	Active Site	Nonionic Membrane	Ionic Membrane
Stanley and Quinn (1987)[11]	TBAB	PTFE	
Grigoropoulou et al. (2001)[12]	TBAHS	PTFE	
Okahata and Ariga (1986)[14]	Onium group $(C_4H_9)_3CH_2XC1$		Poly ultrathin nylon
Yadav and Mehta (1993)[13]	Onium group $(C_4H_9)_3CH_2XCl$		Poly ultrathin nylon
This study	pyridinium group		Poly(MS-*co*-S)

zyl alcohols using a porous polytetrafluoroethylene (PTFE) membrane to separate the aqueous and organic phases using tetrabutylammonium hydrogen sulfate (TBAHS) as the homogeneous catalyst. As mentioned in the above experimental results, these membrane configurations do not actually aid in the separation of the catalyst from the reaction matrix. The catalyst was not immobilized in the membrane. Yadav and Mehta[13] presented the theoretical and experimental analysis of capsule membrane phase-transfer catalysis for alkaline hydrolysis of benzyl chloride to benzyl alcohol. Okahata and Ariga[14] reported the reaction of sodium azide with benzyl bromide in the presence of a capsule membrane with pendant quaternary ammonium groups and polyethylene glycol groups on the outside. However, the capsule membrane is not suitable for direct scale-up to the industrial level because of the inconveniences of working with capsules.

The applications of a Langmuir–Hinshelwood adsorption mechanism to a triphase catalytic system were attempted by Yadav and Mistry[15] for the oxidation of benzyl chloride to benzaldehyde with hydrogen peroxide, using a system with a capsule-membrane Pt catalyst (the model was reduced to a simple single-parameter expression when used to fit the experimental data); and by Satrio et al.[16] for the nucleophilic substitution of octyl bromide with potassium acetate system in the presence of polymer-supported (styrene-*co*-chloromethylstyrene) resin with functional group tributylmethylammonium chloride. The reaction system was described by a model of two or three parameters to fit the experimental data. The purpose of this paper is to combine the studies of membrane-reactor and phase-transfer catalysis. The membrane was used to stabilize the aqueous/organic interface at a fixed position; moreover, the quaternary ammonium ion in the membrane was used as the catalyst to participate directly in the reaction system, and so it can also separate the product and reactants at the same time. A theoretical model is also presented.

Although many researchers[17-19] studied the synthesis of allyl phenyl ether by phase-transfer catalysis, until now no studies have used it in a membrane reactor. One of the objectives of the present study was to carry out allylation of phenol in an ion-exchange membrane reactor, compared with an ionic membrane, a nonionic membrane, and a soluble phase-transfer catalyst to determine the characteristics of the membrane and its reaction in the reactor. The operating conditions for this investigation include molar ratio of reactants; agitation rate; and kinds of solvents, reaction temperatures, and membranes.

Experimental

Materials

Allyl bromide (RBr, 99.5%, Fluka), phenol (RDH, 99%), chloromethylstyrene (Aldrich, 97%), tetra-*n*-butyl ammonium bromide (TBAB, 99%, Fluka), and other reagents are all expanded chemicals. The hydrophilic VVLP membrane (Millipore Co.) had a mean thickness of 125 μm, an average pore size of 0.1 μm, and a typical porosity of 75%. The anion-exchange membrane A172, obtained from Asahi Chemical Industrial Co. Ltd. (Japan), had the following characteristics: thickness, 0.12–0.15 mm; ion-exchange capacity, 1.8–1.9 mol/g dry membrane; water content, 24–25%; electrical resistance, 1.7–20 Ω-cm^2; type, mono anion permselectivity membrane; and reinforcement, PP fabric. The molecular structure of the A172membrane with pyridinium chloride is expressed in the scheme below.

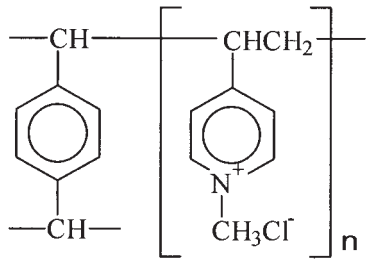

Characterization of A172 membrane

The procedure for determining the imbibed solvent composition of the membrane is presented in the following section. A 50-cm^3 beak served as the testing apparatus. A172 membrane was washed with deionized water, whose external liquid phase was removed using paper. Known quantities of the membrane (2×2 cm^2), organic solvent (dichloroethane), and allyl bromide were added to the flask, which was immersed in a thermostatic constant-temperature (25°C) water-bath shaker. The shaker was agitated at 150 rpm. The shaking was carried out for an extended period (at least 50 min) to allow the reagents to dissolve in the organic solvent. The amount of allyl bromide in dichloroethane was measured by means of high-performance liquid chromatography (HPLC; Shimadzu LC-10A). The imbibed water content in the membrane was obtained by subtracting the amount of wet membrane from that of dry membrane.

The membrane was immersed in deionized water (or dichlo-

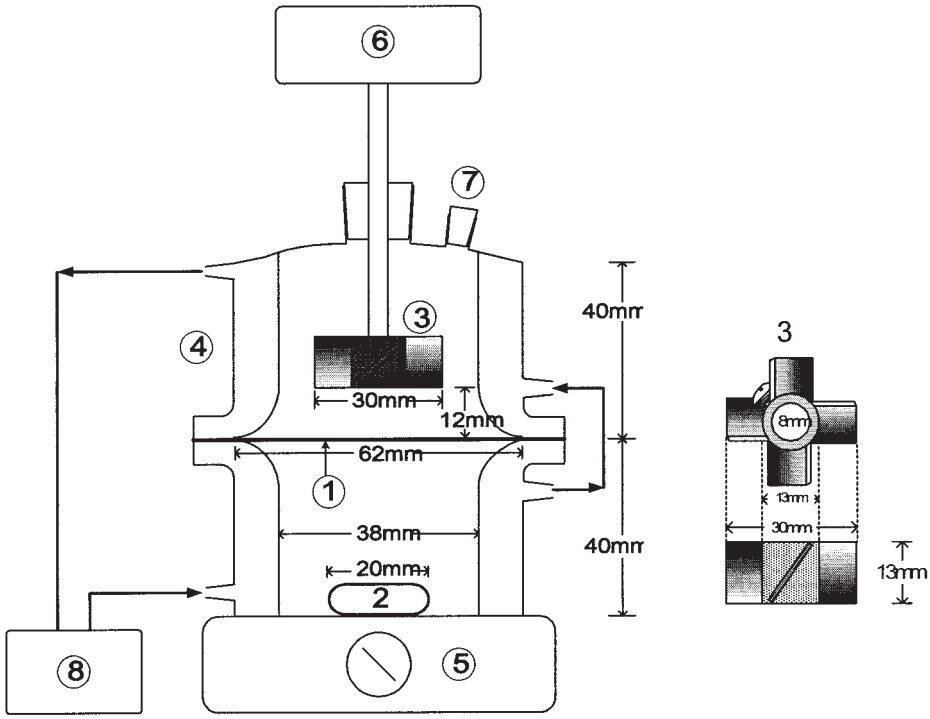

Figure 1. Membrane reactor.

1: Membrane; 2: Teflon stir bar; 3: stainless stirrer; 4: membrane reactor; 5: magnetic stirrer; 6: mechanical stirrer; 7: sampling point; 8: cooling circulator bath.

roethane) for 3 days, after which its surface moisture was wiped. Thicknesses of wet A172 membranes in water and dichloroethane were 0.133 and 0.133 mm, respectively, measured by means of microscopic instrument. Then, this wet membrane was dried at a fixed temperature of 60°C until achieving a constant weight. The thickness of the dry A172 membrane was 0.12 mm. The linear swelling of wet to dry A172 membrane was 11.1%, a finding that demonstrates that the swelling degree of the membrane did not change either in water or dichloroethane. The imbibed water content in the other A172 membrane was 25.5%. However, the imbibed amount of allyl bromide measured was not obtained in the membrane. Thus, the A172 membrane of Br^- form was a hydrophilic membrane and did not imbibe the organic reactant allyl bromide into the membrane.

Exchange between phenolate ion and bromide ion in A172 membrane

First, the counterion in the A172 membrane was exchanged from the Cl^- form to the Br^- form because sodium bromide was a by-product in this study. A 200-cm^3 funnel equipped with a fritted disk served as the exchanging apparatus. A known quantity (0.00302 m^2) of A172 membrane was plated onto the fritted disk, and then 1 N NaBr solution (200 cm^3) was introduced into the funnel. The NaBr solution was removed from the membrane under reduced pressure by using a water aspirator. After the exchanging procedure, the membrane was charged to a flask, which contained 1 N NaBr solution.

Second, the counterion in the A172 membrane was exchanged from the Br^- form to the PhO^- form. A known quantity of sodium phenolate and water (55 cm^3) was prepared and introduced into a beaker (100 cm^3) and thermostated at the desired temperature (65°C). The agitation rate was 400 rpm with a magnetic stirrer. The A172 membrane with bromide ion was obtained from a 1 N NaBr solution, and washed three times with deionized water. The external water was wiped with a blotting paper. Then, the membrane was introduced into the beaker to start the exchange reaction. An aliquot sample (0.2 cm^3) was withdrawn from the solution at selected time intervals. The content of phenolate ion in the aqueous solution was quantitatively analyzed by means of HPLC.

Finally, the exchanging procedure of A172 membrane from the PhO^- form to the Br^- form was identical to that from the Br^- form to the PhO^- form.

Kinetics of membrane-based permeation stirred cell

The experimental apparatus of membrane-based (or without membrane) stirred reactor is shown in Figure 1. It was thermostated by an external circulatory bath to maintain an isothermal condition. The lower organic phase was stirred with a magnetic stirrer, whereas the aqueous phase was stirred with a flat-bladed Teflon stirrer. An aqueous solution (55 cm^3) of sodium hydroxide (mole ratio of NaOH to phenol = 1.67) and phenol (0–0.35 kmol/m^3) was prepared and introduced into the membrane reactor, which was thermostated at the desired temperature (65°C). The membrane was wetted by aqueous phase before the reaction, and then introduced into the reactor. Measured quantities of allyl bromide (0.064–2.36 kmol/m^3), dichloroethane (55 cm^3), and diphenyl ether (internal standard) were prepared and introduced into the reactor and also thermostated at the desired temperature. Two reaction cases of organic reactant (allyl bromide) in excess and aqueous reactant

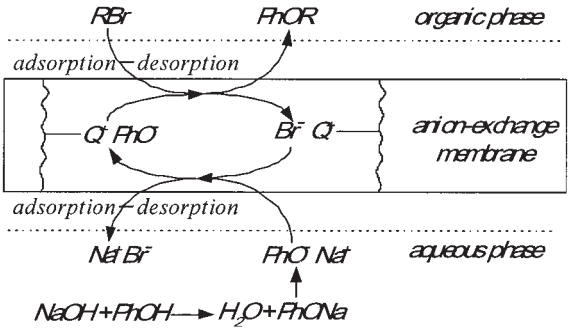

Figure 2. Mechanism of membrane reaction.

(phenol) in excess were individually investigated to determine the reactive performance of A172 membrane. The interfical area between the two phases was 3.02×10^{-3} m^2. The reaction temperature was operated at 65°C, and it did not reduce the reaction rate even after repeating four reaction runs; that is to say, the active site will not fall off after reaction or at high temperature.

For a kinetic run, an aliquot sample was withdrawn from the reaction solution at selected time intervals. The sample (0.1 cm^3) was immediately added to dichloroethane (0.3 cm^3) to quench the reaction. The organic phase content was then quantitatively analyzed by means of HPLC (Shimadzu LC-10A) using the method of internal standard. The accuracy of these analytical techniques was within 2–3% and the data were correctly reproduced within 5% of the values reported in this work.

Mathematical Modeling

In a triphase reaction, the overall kinetic cycle can be broken down into two steps by virtue of the presence of two practically insoluble liquid phases: (1) a chemical conversion step in which the active catalyst sites (Q^+ with phenolate ions, Q^+PhO^-) react with allyl bromide (RBr), to produce allyl phenyl ether (PhOR), and the other active catalyst site of the Br^- form (Q^+Br^-); and (2) an ion-exchange step in which the attached catalyst sites are in contact with the aqueous phase (Figure 2). Two reactions are described as follows:

(1) Organic substitution reaction step

$$RBr + Q^+PhO^- \rightarrow PhOR + Q^+Br^- \tag{1}$$

(2) Aqueous ion-exchange reaction step of phenolate ion (PhO^-) and bromide ion (Br^-)

$$PhO^- + Q^+Br^- \rightleftharpoons Q^+PhO^- + Br^- \tag{2}$$

Assuming that the reversible ion-exchange reaction step can be described by the Langmuir–Hinshelwood adsorption/desorption hypothesis and the formation of a transitional site $PhO^-\cdot Q^+\cdot Br^-$ between the forward and backward reaction steps (Eq. 2), which was established rather rapidly, the ion-exchange reaction in the membrane can be separated into two reactions as follows

$$PhO^- + Q^+Br^- \underset{k_{Ph2}}{\overset{k_{Ph1}}{\rightleftharpoons}} PhO^-\cdot Q^+\cdot Br^- \tag{3}$$

$$Br^- + Q^+PhO^- \underset{k_{Br2}}{\overset{k_{Br1}}{\rightleftharpoons}} PhO^-\cdot Q^+\cdot Br^- \tag{4}$$

Similarly, assuming the formation of a transitional site $Q^+PhO^-\cdot RBr$ in the organic reaction of Q^+PhO^- with RBr, the organic reaction can be expressed as

$$RBr + Q^+PhO^- \underset{k_{RBr2}}{\overset{k_{RBr1}}{\rightleftharpoons}} Q^+\cdot PhO^-\cdot RBr \tag{5}$$

$$Q^+PhO^-\cdot RBr \xrightarrow{k_{PR}} Q^+Br^- + PhOR \tag{6}$$

On the basis of Eqs. 1–6 and Langmuir–Hinshelwood kinetics, the balance equations for Q^+Br^-, Q^+PhO^-, and $Q^+PhO^-\cdot RBr$ are

$$\frac{V}{A}\frac{d[Q^+Br^-]}{dt} = -k_{Ph1}[PhO^-]\theta_{Br}\frac{\lambda M_c}{A} + k_{Ph2}\theta_{PB}\frac{\lambda M_c}{A} \tag{7}$$

$$\frac{V}{A}\frac{d[Q^+PhO^-]}{dt} = -k_{Br1}[Br^-]\theta_P\frac{\lambda M_c}{A} + k_{Br2}\theta_{PB}\frac{\lambda M_c}{A} - k_{RBr1}[RBr](1-\theta_{PR})\theta_P\frac{\lambda M_c}{A} + k_{RBr2}\theta_{PR}\theta_P\frac{\lambda M_c}{A} \tag{8}$$

$$\frac{V}{A}\frac{d[Q^+PhO^-\cdot RBr]}{dt} = -k_{RBr1}[RBr](1-\theta_{PR})\theta_P\frac{\lambda M_c}{A} - k_{RBr2}\theta_{PR}\theta_P\frac{\lambda M_c}{A} - k_{PR}\theta_{PR}\theta_P\frac{\lambda M_c}{A} \tag{9}$$

and the rate expression of the organic reaction is

$$r_R = k_{PR}[Q^+PhO^-\cdot RBr] = k_{PR}\theta_{PR}\theta_P\frac{\lambda M_c}{A} \tag{10}$$

where the the fractions of the monolayer densities θ_P, θ_{Br}, and θ_{PB} are defined by the coverages of Q^+ absorbed PhO^-, Br^-, and $PhO^-\cdot Q^+\cdot Br$, respectively; θ_{PR} is defined by the coverage of Q^+PhO^- attached to RBr (Eq. 6); A denotes the interfical area between the membrane and the liquid phase; M_c denotes the total quantity of active catalyst site; and λ is the fraction of effective active site. The total monolayer density is

$$1 = \theta_P + \theta_{Br} + \theta_{PB} \tag{11}$$

Assuming that the species of Q^+Br^-, Q^+PhO^-, and $Q^+PhO^-\cdot RBr$ are in the pseudo-steady-state condition during the reaction, the following expressions hold

$$\frac{V}{A}\frac{d[Q^+Br^-]}{dt} \approx 0 \tag{12}$$

$$\frac{V}{A}\frac{d[Q^+PhO^-]}{dt} \approx 0 \tag{13}$$

$$\frac{V}{A}\frac{d[Q^+PhO^- \cdot RBr]}{dt} \approx 0 \tag{14}$$

The θ_p and θ_{PR} calculated from Eqs. 7–8 and 11–14 are given as

$$\theta_P = \frac{K_{Ph}[PhO^-]}{(1 + K_{Br}[Br^-] + K_{PRBr})K_{Ph}[PhO^-] + K_{Br}[Br^-] + K_{PRBr}} \tag{15}$$

and

$$\theta_{PR} = \frac{[RBr]}{[RBr] + C_M} \quad C_M = \frac{k_{RBr2} + k_{PR}}{k_{RBr1}} \tag{16}$$

where K_{Ph} ($= k_{Ph1}/k_{Ph2}$) and K_{Br} ($=k_{Br1}/k_{Br2}$) are the equilibrium attachment/detachment constants for PhO^- and Br^- anion; and K_{PRBr} ($=k_{PR}\theta_{PR}/k_{Br2}$) is the ratio of consumption rate to formation rate for Q^+PhO^-.

When the consumption rate for Q^+PhO^- is smaller than the formation rate for Q^+PhO^- (that is, $K_{PRBr} \ll 1$) during the reaction, the organic reaction rate (Eq. 6) is a rate-determining state. From Eqs. 10, 15, and 16, the formation rate for the product can be written as

$$r_R = k_{PR}\left(\frac{[RBr]}{[RBr] + C_M}\right) \times \left(\frac{K_{Ph}[PhO^-]}{(1 + K_{Br}[Br^-] + K_{PRBr})K_{Ph}[PhO^-] + K_{Br}[Br^-] + K_{PRBr}}\right) \times \frac{\lambda M_c}{A} \tag{17}$$

When $1 \gg (K_{Br}[Br^-] + K_{PRBr})$, Eq. 17 can be rewritten as

$$r_R = k_{PR}\left(\frac{[RBr]}{[RBr] + C_M}\right) \times \left(\frac{[PhO^-]}{[PhO^-] + Br^-]/K^{sel}_{Br^-/PhO^-} + K_{PRBr}/K_{ph}}\right)\frac{\lambda M_c}{A} \tag{18}$$

where the equilibrium selectivity constant of PhO^- to Br^- is defined as[20]

$$K^{sel}_{Br^-/PhO^-} = \frac{K_{Ph}}{K_{Br}} = \frac{[Q^+PhO^-][Br^-]}{[Q^+Br^-][PhO^-]}\frac{\gamma_{Q^+PhO^-}\gamma_{Br^-}}{\gamma_{Q^+Br^-}\gamma_{PhO^-}} \tag{19}$$

Equation 18 can be used to estimate the parameters [k_{PR}, C_M, $K^{sel}_{Br^-}/PhO^-$, and $K_{PRBr}/(\theta_{PR}\cdot K_{Ph})$] for providing the experimental data when all active sites were the effective active site, that is, $\lambda = 1$. The computational strategy to estimate the parameters from Eq. 18 is

(1) First, when the concentration of PhO^- is larger, the reaction order for PhO^- is zero and the rate expression becomes

$$r_R = k_{PR}\left(\frac{[RBr]}{[RBr] + C_M}\right)\frac{M_c}{A} \tag{20}$$

According to Eq. 20 and the experiment result for different [RBr] values, the parameters k_{PR} and C_M are determined.

(2) The parameters k_{PR} and C_M obtained in step (1) were substituted into Eq. 18. The parameters $K^{sel}_{Br^-}/PhO^-$ and $K_{PRBr}/(\theta_{PR}\cdot K_{Ph})$ can also be calculated at different Br^- concentrations.

(3) The estimated parameters k_{PR}, C_M, $K^{sel}_{Br^-}/PhO^-$, and $K_{PRBr}/(\theta_{PR}\cdot K_{Ph})$ were substituted into Eq. 18 to calculate PhOR. The estimations were compared to satisfy the following condition

$$\frac{PhOR_{evaluated} - PhOR_{exp}}{PhOR_{exp}} < 6\% \tag{21}$$

Results and Discussion

The system chosen for study was the reaction of allyl bromide with phenol, with membrane-supported pyridinium salt as a triphase catalyst in an organic solvent/alkaline solution. In previous investigations,[17,18] the formation kinetics of allyl phenyl ether using tetra-*n*-butyl ammonium bromide (TBAB) as a liquid–liquid phase transfer catalyst was studied.

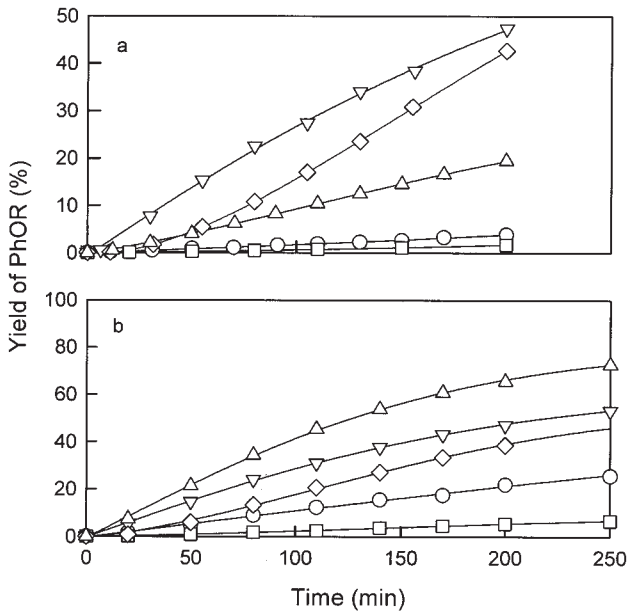

Figure 3. Effect of the types of membranes and without membrane on the yield of PhOR.

Reaction conditions: 65°C, 100 rpm; H_2O: 55 cm^3, $C_2H_4Cl_2$: 55 cm^3. (a) Aqueous reactant excess: 0.004 mol of C_3H_5Br, 0.0125 mol of PhONa; (b) organic reactant excess: 0.03 mol of C_3H_5Br, 0.004 mol of PhoNa. (○) without both membrane and catalyst; (▽) without membrane, and TBAB 0.7 mmol; (□) VVLP membrane, and without catalyst; (◇) VVLP membrane, and TBAB 0.7 mmol; (△) Q^+ in A172 membrane: 0.7 mmol.

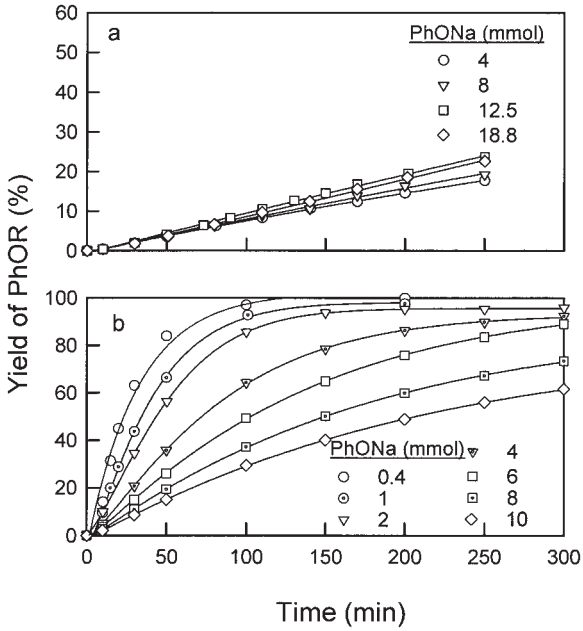

Figure 4. Effect of amount of PhONa on the yield of PhOR.

Reaction conditions: 65°C, 100 rpm; H_2O: 55 cm^3, $C_2H_4Cl_2$: 55 cm^3. (a) Aqueous reactant excess: 0.004 mol of C_3H_5Br; (b) organic reactant excess: 0.03 mol of C_3H_5Br, phenol: NaOH = 1:1.67.

Capability of membrane

Figure 3 shows the effect of the nature types of membranes and without membrane on the yield of PhOR. Five reaction conditions were studied to test the performance of membranes in a batch reactor as follows: (i) without both membrane and catalyst; (ii) without membrane, and TBAB 0.7 mmol; (iii) VVLP membrane, and without catalyst; (iv) VVLP membrane, and TBAB 0.7 mmol; and (v) Q^+ in A172 membrane: 0.7 mmol. The VVLP membrane is a hydrophilic and nonionic membrane. All agitation rates were 100 rpm. The two phases were separately stirred without causing either phase to disperse. A flat interface was maintained between the two phases by regulating the speed of the two stirrers. In general, the aqueous reactant usually was in excess to obtain the maximum partition concentration of QOR in the organic phase, and to achieve the maximum reaction rate in a liquid–liquid phase-transfer–catalyzed reaction. If it was conducted to evaluate the performance of membrane, the yields of PhOR are ranked in the following descending order by case: (ii) > (iv) > (v) > (i) > (iii) (Figure 3a). The reaction without membrane in the presence of TBAB was the best among five reaction conditions because its mass-transfer resistance was the smallest. Whether with or without membrane, the yield of PhOR using TBAB as a liquid–liquid phase-transfer catalyst was higher. However, these reactions did not actually aid in the separation of the catalyst from the reaction matrix. The reaction in case (v) was studied with an A172 membrane with pyridinium chloride as catalyst, which is a hydrophilic membrane. The ratio of reaction rate of case (ii) to case (v) was about 2, for a mild mixing condition of 100 rpm. In general, this value is smaller than that of the liquid–liquid PTC reaction using TBAB as the catalyst to the liquid–solid–liquid PTC reaction using quaternary ammonium poly(methylstyrene-*co*-styrene) resin as the catalyst, a value of nearly 5 for a more robust set of mixing reaction conditions.

If the organic reactant was in excess, the yields of PhOR were ranked in the following descending order by case: (v) > (ii) > (iv) > (i) > (iii) (Figure 3b). The reaction rate of case (v) was the best, and larger than that of case (ii). That is, the performance of the reaction with an A172 membrane was larger than that with TBAB (free catalyst) when the organic reactant was in excess. This result demonstrates that the A172 membrane served to localize the aqueous/organic interface and to avoid problems like emulsification of the phases during separation, and the reactivity of the catalyst in A172 membrane was larger than that of TBAB because the role of excess organic reactant offers a substantially reactive microenvironment in the membrane.

In a more robust mixing reaction system, the reaction rate remained almost constant when the agitation rate was in the range of 200 to 800 rpm in the presence of membrane, that is, the external mass-transfer resistance on the membrane could be negligible. Therefore, the agitation rate was set at 400 rpm to allow us to study the kinetic phenomena in the present reaction. Four kinds of solvents (boiling point > 65°C) were used to investigate the effects of the solvents on the formation of allyl phenyl ether. The sequence of reaction rate for solvents is 1,2-dichloroethane > nitrobenzene > chlorobenzene > toluene. Thus, 1,2-dichloroethane was chosen as the organic solvent for kinetic study in this work. Furthermore, the apparent activation energy calculated from the relation of $\ln(r_R)$ vs. $1/T$ was used to explain the reaction reactivity for different reaction conditions. The apparent activation energy of using nonionic membrane obtained was 20.0 kcal/mol in the range of 35 to 65°C for using tetra-*n*-butylammonium bromide as the catalyst in case (iii). For case (v), the apparent activation energy obtained was 14.73 kcal/mol when aqueous reactant was in excess, and it was only 12.86 kcal/mol when organic reactant was in excess. With respect to literature values,[18,21] the apparent

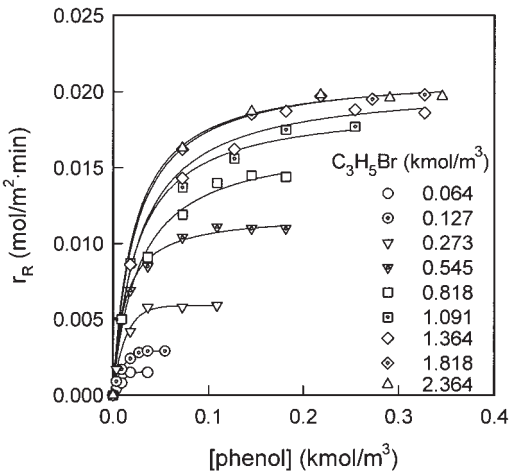

Figure 5. Plot of phenol concentration on the initial reaction rate at different allyl bromide concentrations.

Reaction conditions: 65°C, 400 rpm; H_2O: 55 cm^3, $C_2H_4Cl_2$: 55 cm^3, phenol:NaOH = 1:1.67, Q^+ in A172 membrane: 0.7 mmol.

activation energies of the phenol allylation were 14–16 and 18.6 kcal/mol in the liquid–liquid and the liquid–solid–liquid PTC reactions, respectively.

Two reaction conditions, organic reactant in excess and aqueous reactant in excess, were conducted to test the allylation reactivity using A172 membrane. Figure 4a shows the effect of amount of PhONa with 0.004 mol of C_3H_5Br when the organic reactant was a limiting reactant. The yield of PhOR calculated was based on the amount of C_3H_5Br. The increment of the amount of PhONa slightly increased the yield of PhOR. It is demonstrated that this allylation reaction using A172 membrane to increase the reaction rate is improper when the aqueous phase is in excess, given that A172 membrane is hydrophilic (wetted by the aqueous phase). Figure 4b shows the effect of the amount of PhONa when the organic reactant was in excess with 0.03 mol of C_3H_5Br. The yield of PhOR calculated was based on the amount of PhONa. The formation percentage of PhOR increased with decreasing amount of phenolate ion. This finding demonstrates that the concentration of active sites (Q^+PhO^-) does not remain constant during the course of the reaction. Under an aqueous reactant limiting condition, the yield of allyl phenyl ether could reach beyond 95% under appropriate conditions after a reaction time of 150 min. These results demonstrate that the PTC reaction using A172 membrane as the catalyst prefers to deal with the organic reactant in an excess reaction system.

Modeling of Langmuir–Hinshelwood Kinetics

The formation rate of product r_R was obtained by using the concept of initial rate method, thereby restricting the content of allyl phenyl ether in the aqueous phase to <10%. Figure 5 shows the relationship between the formation rate of product and the concentration of phenolate ion at different concentrations of allyl bromide. The r_R value increased with increasing concentrations of phenolate ion and allyl bromide. The qualitative feature of reaction kinetics is similar to Langmuir–Hinshelwood kinetics. Thus, a mechanism used in traditional heterogeneous catalysis, such as the Langmuir–Hinshelwood adsorption mechanism, attempts to explain this phenomenon. At high phenolate concentration, the r_R value remained constant, and all the active sites may be occupied by phenolate ion.

A definition of $r_{R,max}$ is the maximum formation rate for a certain concentration of phenolate ion. The $r_{R,max}$-value increased with increasing concentration of allyl bromide (Figure 6a). The $r_{R,max}$ value increased when the concentration of allyl bromide increased up to 1.5 kmol/m^3, a finding that reveals that the formation rate increased with increasing adsorption amount of allyl bromide on the membrane surface. The relationship between the required concentration of phenol to achieve $r_{R,max}$ and concentration of allyl bromide is shown in Figure 6b. The required concentration of phenolate ion increased when the concentration of allyl bromide increased. The qualitative feature of reaction kinetics could be described by means of Langmuir–Hinshelwood kinetics.

The $r_{R,max}$ value remained around 0.02 mol/(m^2·min) when the concentration of allyl bomide and phenolated ion were more than 2.0 and 0.2 kmol/m^3, respectively. According to these experimental results, Eqs. 1 to 17 were derived to describe this reaction system. The parameters of k_{PR} and C_M, calculated from Eq. 20 and Figure 6, were 1.53×10^{-3} s^{-1} and

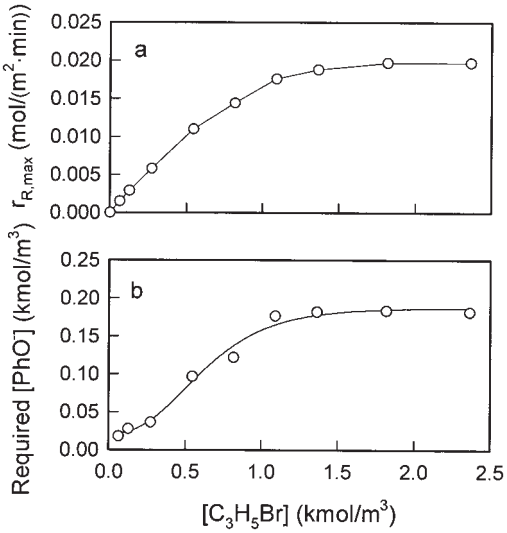

Figure 6. Plots of (a) the maximum initial reaction rate and (b) required concentration of phenolate ion to achieve $r_{R,max}$ vs. allyl bromide concentration.

Reaction conditions are the same as those in Figure 5.

0.485 kmol/m^3, respectively. The turnover number, which is defined as the maximum consumed mole of substrate per catalyst mol per time [$=r_{R,max}/(M_c/A)$], was also 1.53×10^{-3} s^{-1} at 65°C. This finding demonstrates that the order of magnitude corresponds to results reported by Wu[9] using quaternary ammonium polymer-supported resin as the catalyst in the liquid–solid–liquid PTC reaction. Based on Figure 7, the parameters $K^{sel}_{Br^-}/PhO^-$ and $K_{PRBr}/(\theta_{PR} \cdot K_{Ph})$ calculated from Eq. 18 were 0.99 and 0.021 m^3 mol^{-1} s^{-1}, respectively. Because the $K^{sel}_{Br^-}/PhO^-$ is <1, the aqueous ion-exchange reaction in Eq. 2 favors the backward reaction.

Figure 7 shows the effects of concentrations of phenol, allyl bromide, and sodium bromide for experimental results and simulated profiles of fractions of monolayer densities θ_P and θ_{PR} of Q^+PhO^- and $Q^+PhO^- \cdot RBr$, respectively. The computational strategies are described in the section on mathematical modeling. Figures 7a1, b1, and c1 display the estimated trajectories of yield of PhOR for the different concentrations of phenol, ally bromide, and sodium bromide with reaction time. The standard deviations between experimental and simulated results were less than 0.06. The fraction of monolayer densities of Q^+PhO^-, θ_P, were decreased with increasing reaction time because the phenol was a limiting reactant. The value of θ_P increased with increasing concentration of phenol and decreasing concentration of allyl bromide, and was nearly independent of concentration of sodium bromide. Meanwhile, the fraction of monolayer densities of $Q^+PhO^- \cdot RBr$, θ_{PR}, were decreased with increasing reaction time because the phenol was a limiting reactant. The value of θ_{PR} increased with decreasing concentration of phenol and increasing concentration of allyl bromide, and was independent of concentration of sodium bromide. The value of θ_{PR} remained almost constant during the course of the reaction when the ratio of allyl bromide to phenol was more than 10, of which the

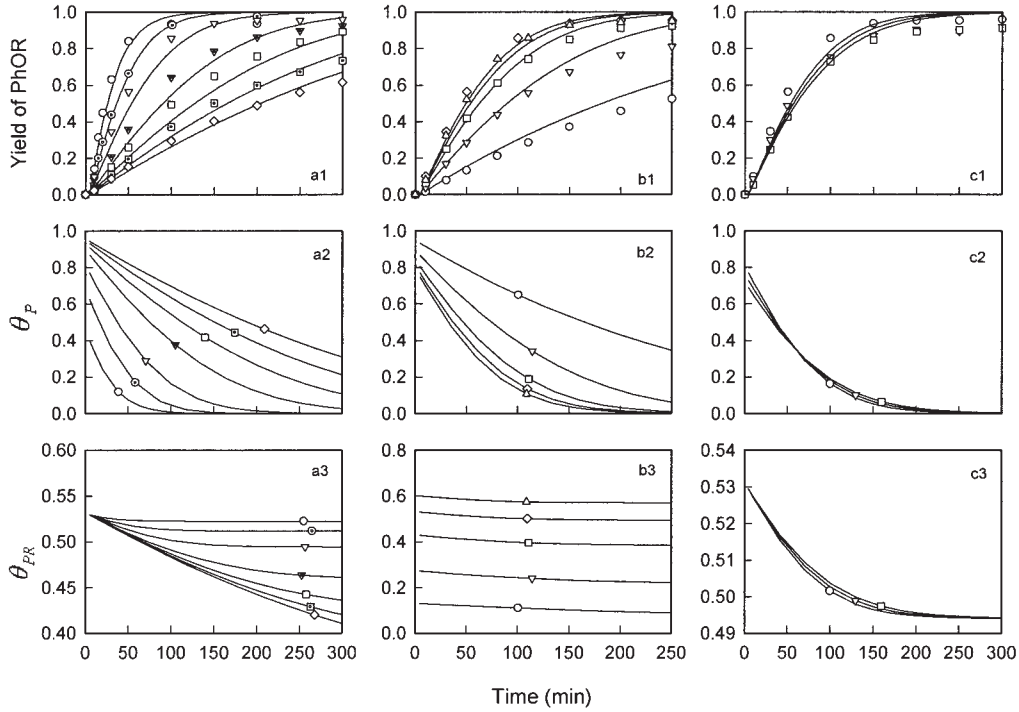

Figure 7. Effects of concentrations of phenol, allyl bromide, and sodium bromide for experimental data and simulated profiles of fractions of monolayer densities θ_P and θ_{PR} of Q^+PhO^- and Q^+PhO^-·RBr, respectively: 65°C, 400 rpm, H_2O = 55 cm^3, $C_2H_4Cl_2$ = 55 cm^3, phenol:NaOH = 1:1.67, Q^+ in A172 membrane = 0.7 mmol.

(a1), (a2), (a3) phenol = (○) 0.4 mmol, (⊙) 1 mmol, (▽) 2 mmol, (▼) 4 mmol, (□) 6 mmol, (⊡) 8 mmol, (◇) 10 mmol, allyl bromide = 30 mmol. (b1), (b2), (b3) allyl bromide = (○) 4 mmol, (▽) 10 mmol, (□) 20 mmol, (◇) 30 mmol, (△) 40 mmol, phenol = 2 mmol. (c1), (c2), (c3) NaBr = (○) 0 mmol, (▽) 0.5 mmol, (□) 1 mmol, allyl bromide = 30 mmol, phenol = 2 mmol.

variation of the θ_{PR} value was <8% in Figure 7a3, and decreased when the ratio of allyl bromide to phenol was <10. All θ_{PR} values in Figures 7a3, b3, and c3 (that is, effective active site or the fraction of the coverage of Q^+PhO^- attached to RBr) are <0.6. These experimental results verify that the reaction rate is influenced by the rate of allyl bromide adsorbed onto the Q^+PhO^-.

Equilibrium and sorption of phenolate ion in membrane

In this allylation system, the phenolate ion simultaneously existed in the aqueous phase, membrane, and organic phase. Figure 8 shows the amounts of phenolate ion existing in the aqueous phase, membrane, and organic phase in the absence of organic reactant, allyl bromide, at different temperatures (25 and 65°C) and different initial amounts of phenolate ion in the aqueous phase during the course of extraction. The sodium phenolate was assumed to be made from phenol and sodium hydroxide (the concentration ratio of phenol to sodium hydroxide was 1/1.67) because the pK_a value of phenol is 9.97. The experimental results demonstrate that the percentage of phenolate ion in the organic phases and extraction rate of phenolate ion from aqueous phase to organic phase increased with increasing temperature. The calculated overall mass-transfer coefficients of phenolate ion from the aqueous phase to the organic phase were 3.7×10^{-6} and 12.4×10^{-6} m s^{-1} at 25 and 65°C, respectively. The order of magnitude of this result is smaller than that of the previous work (10^{-5})[22] for the transfer of different quaternary ammonium salt between two phases. This finding reveals that the permeation resistance of phenolate ion in the A172 membrane was large. The amount of phenolate ion in the membrane increased with the initial amount of phenolate sodium in the aqueous phase. However, the amount of phenolate ion in the membrane was not absolutely increased by increasing temperature when the amount of phenolate ion in the aqeuous phase was <0.7 mmol, and had maximum values in the membrane with reaction time. The amount of phenolate ion in the membrane was reduced when the percentage of phenolate in the organic phase was larger than that in the aqueous phase. It is demonstrated that the ability of adsorbing phenolate ion to exchange bromide ion on the active site of the catalyst in the membrane was unstable, and was smaller than that of adsorbing bromide ion to exchange phenolate ion on the active site of the catalyst. The equilibrium amount of phenolate ion in the membrane increased with increasing initial amount of sodium phenolate in the aqueous phase. The exchange percentage of phenolate ion with bromide ion was 82% when the initial amount of sodium phenolate was 4 mmol (Figure 8d2).

The experimental result in Figure 9 was conducted in the absence of organic reactant and organic solvent. Figure 9a shows the amount of phenolate ion in the membrane on the initial amount of NaBr in the absence of sodium phenolate when the active site was 0.16 mol/m^2 of phenolate ion and 0.07 mol/m^2 of bromide ion. Figure 9b shows the amount of phenolate ion in the membrane on the initial amount of phenolate ion in the absence of sodium bromide when the active site with bromide ion was 0.23 mol/m^2. The equilib-

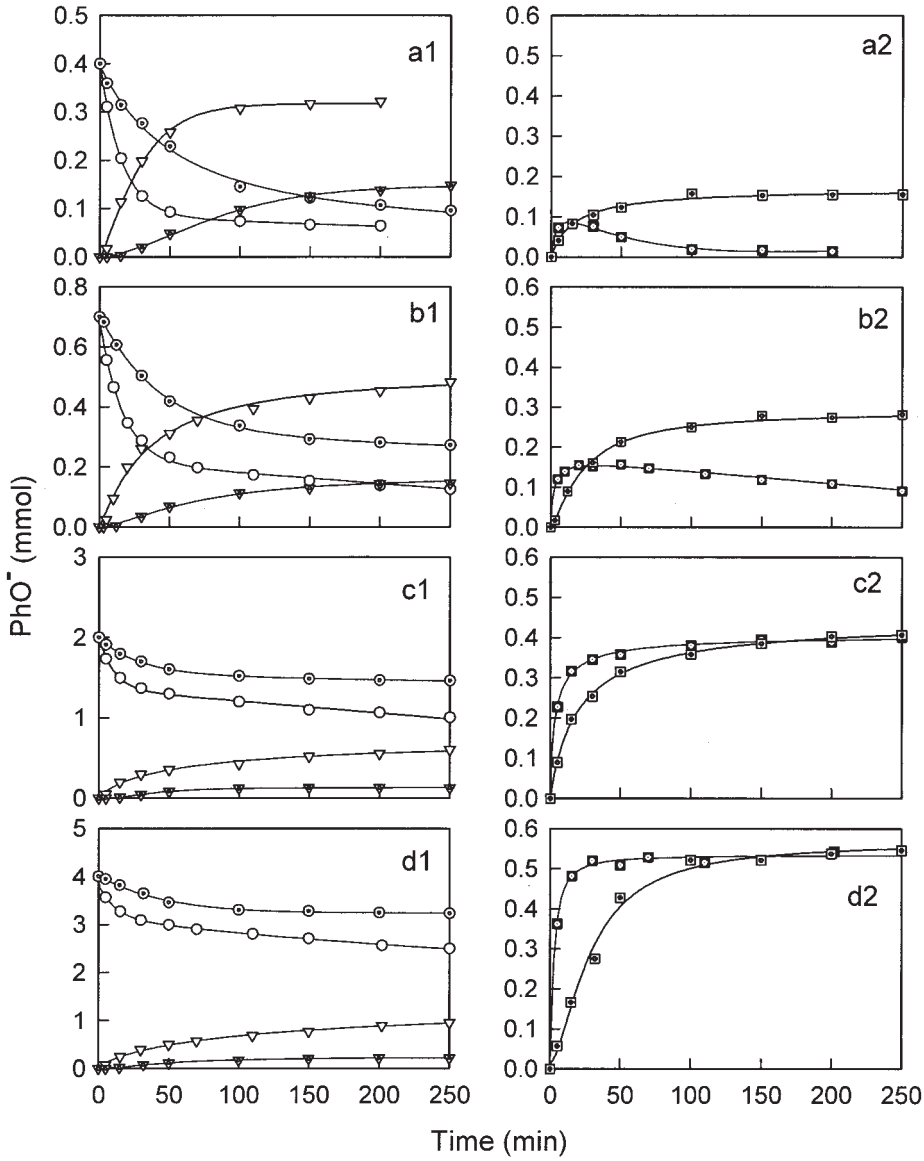

Figure 8. Effects of initial amount of sodium phenolate for the content of phenolate ion in the aqueous phase, organic phase and membrane at different temperatures.

Reaction conditions: 400 rpm, H_2O = 55 cm^3, $C_2H_4Cl_2$ = 55 cm^3, Q^+ in A172 membrane = 0.7 mmol, phenol:NaOH = 1:1.67; phenol: (a1, a2) 0.4 mmol, (b1, b2) 0.7 mmol, (c1, c2) 2 mmol, (d1, d2) 4 mmol; 65°C: (○) aqueous phase, (▽) organic phase, (▪) A172 membrane; 25°C: (⊙) aqueous phase, (▽) organic phase, (⊡) A172 membrane.

rium amount of the catalyst with bromide ion slightly increased with increasing initial amount of NaBr (Figure 9a). The amount of phenolate ion with the active site of the catalyst could be completely exchanged by bromide ion. However, the equilibrium amount of the active site with phenolate ion obtained after 20 min of adsorbing time increased with increasing initial amount of sodium phenolate up to 3 mmol, and after 100 min of adsorbing time decreased when the value was >3 mmol (Figure 9b). The amount of bromide ion with the active site of the catalyst was not completely exchanged by phenolate ion. This finding demonstrates that the high concentration of phenolate ion in the aqueous solution changed the environment of phenolate ion adorbed on the active site of the catalyst; and the phenolate ion in the catalyst was exchanged by bromide ion. According to the experimental result in Figure 9b, the selectivity coefficients $K^{sel}_{Br^-}/PhO^-$ were calculated by Eq. 19, assuming that the activity coefficient was unity, and are shown in Figure 10. The value of $K^{sel}_{Br^-}/PhO^-$ is <1, and is around 0.8 when the initial amount of sodium phenolate is <1.5 mmol. The experimental result corresponds to the simulated result as mentioned above.

According to Eqs. 3 and 4, the adsorbing rates of phenolate ion (or bromide ion) in the membrane are simply given as

$$\frac{V}{A}\frac{d[PhO^-]}{dt} = -k_{Ph1}[Br^-]\theta_{Br}\frac{\lambda M_c}{A} \tag{22}$$

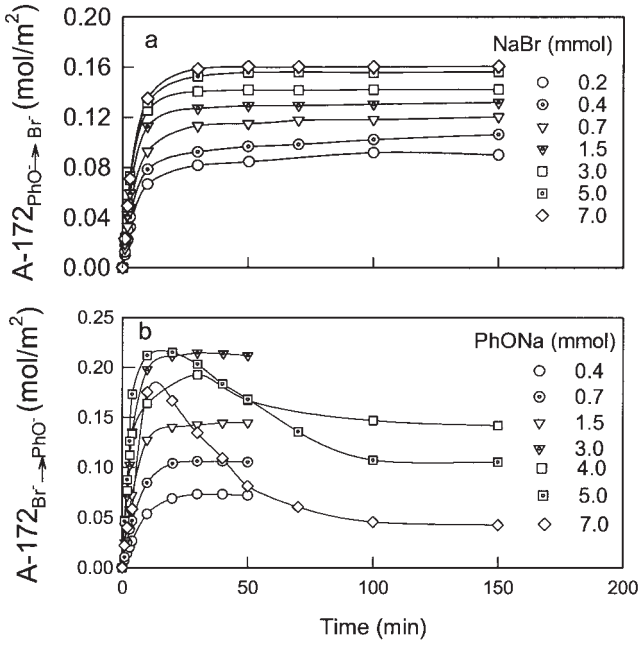

Figure 9. Effects of (a) initial amount of (b) sodium bromide and sodium phenolate for the contents of (a) phenolate ion and (b) bromide ion in the membrane, respectively.

Reaction conditions: 65°C, 400 rpm, Q^+ in A172 membrane (30.2 cm^2): 0.7 mmol, aqueous solution: 55 cm^3.

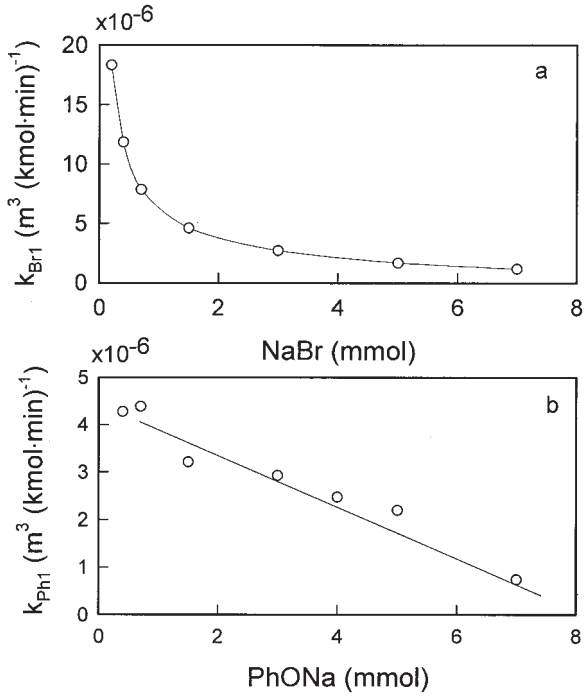

Figure 11. Plots of (a) initial amount of sodium bromide vs. k_{Br1} and (b) sodium phenolate vs. k_{Ph1}.

Reaction conditions are the same as those in Figure 9.

and

$$\frac{V}{A}\frac{d[\mathrm{PhO}^-]}{dt} = -k_{Br1}[\mathrm{Br}^-]\theta_P\frac{\lambda M_c}{A} \tag{23}$$

Using the concept of the initial rate approach and the experimental results in Figure 9, the parameters k_{Ph1} and k_{Br1} were calculated and are shown in Figure 11. The value of k_{Ph1} (or k_{Br1}) decreased with increasing initial amount of sodium phenolate (or sodium bromide). k_{Ph1} values were smaller than k_{Br1} values. This result verifies that the active site of the catalyst in the membrane is more favorable toward adsorbing bromide ion than toward adsorbing phenolate ion. The ratio of k_{Ph1} to k_{Br1} calculated was also <1. This result verifies again that the adsorption of the active site in the membrane with adsorbing the bromide ion is larger than that with adsorbing the phenolate ion.

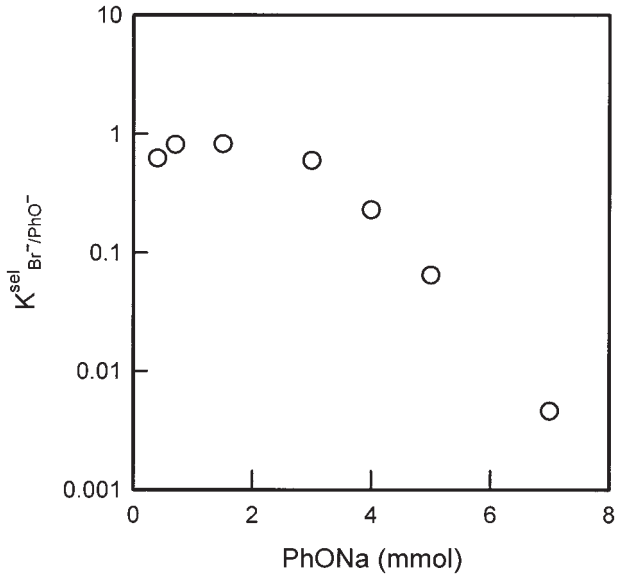

Figure 10. Plot of selectivity coefficient vs. initial amount of sodium phenolate.

Reaction conditions are the same as those in Figure 9.

Conclusions

The reaction mechanism and mathematical model of allylation of phenol in a liquid-membrane–liquid reaction system was investigated. The reaction kinetics was well described by the Langmuir–Hinshelwood theory. The active site in the A172 membrane is a pyridinium group, which is different from that of the traditional phase-transfer catalyst with butyl ammonium group. The catalyst with methyl group was inappropriate as a liquid catalyst for application in a liquid–liquid phase-transfer–catalytic reaction and as a solid catalyst, immobilized in polymer-supported resin for application in a liquid–solid–liquid PTC reaction, because the catalyst was hydrophilic. However, the yield of the reaction could obtain significant results when the catalyst with pyridinium group was immobilized in the membrane, especially when the organic reactant was in excess. The membrane module, used as a combination reactor and separator unit, where the membrane did not participate in carrying out the PTC reaction, was also used to simultaneously and selectively recover the organic product. This experimental result is

valuable for solving the problem of environmental wastewater, which involves organic compounds.

Acknowledgments

The authors thank the National Science Council of the Republic of China for financial support of this research under Grant NSC 89-2214-E155-006.

Notation

A = interfacial area between membrane and liquid phase, m^2
k_{Br1} = forward reaction rate constant of Br^- with Q^+PhO^- in the aqueous phase, $(kmol/m^3 \cdot s)^{-1}$
$k_{Br}2$ = backward reaction rate constant of Br^- with Q^+PhO^- in the aqueous phase, $(kmol/m^3 \cdot s)^{-1}$
k_{Ph1} = forward reaction rate constant of PhO^- with Q^+Br^- in the aqueous phase, $(kmol/m^3 \cdot s)^{-1}$
k_{Ph2} = backward reaction rate constant of PhO^- with Q^+Br^- in the aqueous phase, $(kmol/m^3 \cdot s)^{-1}$
k_{PR} = rate constant for the substitution reaction in the organic phase, $(kmol/m^3 \cdot s)^{-1}$
k_{RBr1} = forward reaction rate constant of RBr with $Q^+ \cdot PhO^- \cdot RBr$ in the aqueous phase, $(kmol/m^3 \cdot s)^{-1}$
k_{RBr2} = backward reaction rate constant of RBr with $Q^+ \cdot PhO^- \cdot RBr$ in the aqueous phase, $(kmol/m^3 \cdot s)^{-1}$
K_{Br^-} = equilibrium constant of k_{Br1}/k_{Br2}, defined by Eq. 3
K_{Ph} = equilibrium constant of k_{Ph1}/k_{Ph2}, defined by Eq. 4
K_{PRBr} = equilibrium constant of k_{RBr1}/k_{RBr2}, defined by Eq. 5
K_{Br}^-/PhO_-^{sel} = selectivity constant of Br^- to PhO^-, defined by Eq. 19
M_c = total quantity of active catalyst site, mol
MS = methylstyrene
Q^+ = active catalyst site
RBr = organic reactant
S = styrene
$PhOR$ = aqueous reactant
PTFE = polytetrafluoroethylene
t = reaction time, s
T = temperature, K
TBAB = tetra-*n*-butylammonium bromide
TBAHS = tetra-*n*-butylammonium hydrogen sulfate
V = volume of aqueous solution, m^3
X = N or P

Greek letters

θ_{Br} = fraction of the monolayer density defined as the coverage of Q^+Br^- attached to RBr
θ_P = fraction of the monolayer density defined as the coverage of Q^+PhO^- attached to RBr
θ_{PR} = fraction of the monolayer density defined as the coverage of $Q^+ \cdot PhO^- \cdot RBr$ attached to RBr
λ = fraction of effective active site

Literature Cited

1. Starks CM, Liotta CL, Halpern M. *Phase-Transfer Catalysis, Fundamentals, Applications, and Industrial Perspectives*. New York, NY: Chapman & Hall; 1994.
2. Yang HM, Wu HS. *Interfacial Mechanism and Kinetics of Phase-Transfer Catalysis in Interfacial Catalysis*. Volkov AG, ed. New York, NY: Marcel Dekker; 2002;285-353.
3. Dehmlow VV, Dehmlow SS. *Phase Transfer Catalysis*. Weinheim, Germany: Verlag Chemie; 1993.
4. Ragaini V, Saed G. Heterogenized phase transfer catalysts in a fixed-bed reactor kinetic study of a nucleophilic substitution. Z *Phys Chem NF.* 1980;119:117-128.
5. Ragaini V, Verzella G, Ghignone A, Colombo G. Fixed-bed reactors for phase-transfer catalysis. A study of a liquid–liquid–solid reaction. *Ind Eng Chem Process Des Dev.* 1986;25:878-885.
6. Ragaini V, Colombo G, Barzhagi P. Phenylacetonitrile alkylation with different phase-transfer catalysts in continuous flow and batch reactors. *Ind Eng Chem Res.* 1988;27:1382-1387.
7. Ragaini V, Colombo G, Barzhagi P, Chiellini E, D'Antone S. Phase transfer alkylation of phenylacetonitrile in prototype reactors under magnetic or ultrasound mixing conditions: 2. Kinetic modeling. *Ind Eng Chem Res.* 1990;29:924-925.
8. Schlunt P, Chau PC. The reaction kinetics of a polymer-bound phase transfer catalyst in a novel cyclic slurry reactor. *J Catal.* 1986;102: 348-356.
9. Wu HS, Wang CS. Liquid–solid–liquid phase-transfer catalysis in sequential phosphazene reaction: Kinetic investigation and reactor design. *Chem Eng Sci.* 2003;58:3523-3534.
10. Zaspailis VT, Van Praag W, Keizer K, Van Ommen JG, Ross JRH, Burggraaf AJ. Reaction of methanol over catalytically active alumina membranes. *Appl Catal.* 1991;74:205-209.
11. Stanley TJ, Quinn JA. Phase transfer catalysis in a membrane reactor. *Chem Eng Sci.* 1987;42:2313-2324.
12. Grigoropoulou G, Clark JH, Hall DW, Scott K. The selective oxidation of benzyl alcohols in a membrane reactor. *Chem Commun*. 2001;547-548.
13. Yadav GD, Mehta PH. Theoretical and experimental analysis of capsule membrane phase transfer catalysis: Selective alkaline hydrolysis of benzyl chloride to benzyl alcohol. *Catal Lett.* 1993;21:391-403.
14. Okahata Y, Ariga K. A new type of phase-transfer catalysts (PTC). reaction of substrates in the inner organic phase with the outer aqueous anions catalyzed by PTC grafted on the capsule membrane. *J Org Chem.* 1986;51:5064-5068.
15. Yadav GD, Mistry CK. A new model of capsule membrane phase transfer catalysis for oxidation of benzyl chloride to benzaldehyde with hydrogen peroxide. *J Mol Catal A Chem*. 1995;102:67-72.
16. Satrio JAB, Glatzer HJ, Doraiswamy LK. Triphase catalysis: A rigorous mechanistic model for nucleophilic substitution reactions based on a modified Langmuir–Hinshelwood/Eley–Rideal approach. *Chem Eng Sci.* 2000;55:5013-5033.
17. Mckillop A, Fiaud JC, Hug RP. The use of phase transfer catalysis for the synthesis of phenol ether. *Tetrahedron.* 1974;30:1379-1382.
18. Wu HS, Lai JJ. Product selectivity of phenoxide allylation in phase-transfer catalyzed reaction system. *J Chin Inst Chem Eng.* 1995;26: 277-283.
19. Wang ML, Chang KR. Reaction mechanism and kinetics of the allylation of phenoxide in the *n*-decane/H_2O-PEG-400 system. *Ind Eng Chem Res.* 1991;30:2378-2383.
20. Helfferich F. *Ion Exchange*. New York, NY: McGraw-Hill; 1962.
21. Yang HM, Wu CM. Phase-transfer catalyzed allylation of sodium phenoxide in a solid–liquid system. *J Mol Catal A Chem.* 2000;153: 83-91.
22. Wu HS, Liu CB, Lin YH. Extraction of halide quaternary salts in an organic solvent/water system: Hydrodynamics and mass transfer. *Can J Chem Eng.* 2002;80:421-431.

Manuscript received Aug. 19, 2003, and revision received July 5, 2004.